Submitted to ApJ, 3 March 2014
Preprint typeset using LaTeX style emulateapj v. 11/10/09

ON THE LACK OF CORRELATION BETWEEN Mg II 2796, 2803 Å AND LYMAN α EMISSION IN LENSED STAR-FORMING GALAXIES

J. R. Rigby[1], M. B. Bayliss[2,3] M. D. Gladders[4,5], K. Sharon[6], E. Wuyts[7], & H. Dahle[8]

Submitted to ApJ, 3 March 2014

ABSTRACT

We examine the Mg II 2796, 2803 Å, Lyman α, and nebular line emission in five bright star-forming galaxies at $1.66 < z < 1.91$ that have been gravitationally lensed by foreground galaxy clusters. All five galaxies show prominent Mg II emission and absorption in a P Cygni profile. We find no correlation between the equivalent widths of Mg II and Lyman α emission. The Mg II emission has a broader range of velocities than do the nebular emission line profiles; the Mg II emission is redshifted with respect to systemic by 100 to 200 km s^{-1}. When present, Lyman α is even more redshifted. The reddest components of Mg II and Lyman α emission have tails to 500–600 km s^{-1}, implying a strong outflow. The lack of correlation in the Mg II and Lyman α equivalent widths, the differing velocity profiles, and the high ratios of Mg II to nebular line fluxes together suggest that the bulk of Mg II emission does not ultimately arise as nebular line emission, but may instead be reprocessed stellar continuum emission.

Subject headings: galaxies: star formation — techniques: spectroscopic — ISM: jets and outflows — gravitational lensing: strong

1. INTRODUCTION

It has recently become evident that the spectra of distant galaxies frequently show Mg II 2796, 2803 in the classic P Cygni profile of redshifted emission and blueshifted absorption. Such emission is notably absent in $z = 0$ analogues.

Weiner et al. (2009) reported the first detection of Mg II emission in distant galaxies, finding Mg II emission with a P Cygni profile in the stacked spectra of z=1.4 galaxies. They attributed this emission to a small fraction (50 out of 1400) of the sample, "most probably from narrow-line active galactic nuclei", in part because of a high-velocity tail in the emission line profile. Rubin et al. (2010) repeated this analysis on a lower-redshift (0.7<z<1.5) sample of galaxies, and found Mg II emission in the stack of 468 galaxies, as well as in some individual galaxy spectra. They suggested that this Mg II emission arises not from nuclear accretion, but from resonant scattering in an expanding wind, analogous to the resonant scattering of Lyman alpha.

Rubin et al. (2011) found Mg II emission that extended spatially across at least 7 kpc in a z=0.69 galaxy, which also showed prominent Fe II* fine structure emission. The authors noted that the Fe II* and Mg II kinematics did not resemble those of nebular emission lines. They argued that the Mg II resonant emission and the Fe II* fine structure emission most likely arise via photon scattering in an outflowing wind. Giavalisco et al. (2011) found Mg II and Fe II* emission in a stack of 33 galaxies at z=1.6, and in a stack of 92 galaxies at 1.65<z<2.5. They note that at matched spectral resolution, non-AGN z=0 galaxies show no such Mg II and Fe II* emission (Kinney et al. 1993), except for the Wolf-Rayet galaxy TOL 1924-416. None of the galaxies in the Giavalisco et al. (2011) stacks are detected in 4 Ms of Chandra X-ray integration, which argues against the significant presence of X-ray–luminous AGN.

Erb et al. (2012) showed how common Mg II and Fe II* emission are in 1<z<2 galaxies. Mg II emission is seen in one-third of their sample: 33 of 93 galaxies. Fe II* emission appears even more ubiquitous, appearing in all the stacks of subsamples.

Prochaska et al. (2011) simulate Mg II P Cygni profiles like those observed in these distant galaxies, using a Monte Carlo radiative transfer model that assumes a cool, outflowing wind.

Thus, while the first detections of Mg II emission lines in galaxies were thought to be a rare curiosity with a suspected AGN origin, such emission is now recognized as common in distant star-forming galaxies, though notably absent in z=0 analogues.

In this paper, we examine Mg II emission and absorption from five star-forming galaxies at $1.66 < z < 1.91$ that have been gravitationally lensed by foreground galaxy clusters. While our sample size is much smaller than field samples, lensing magnification has enabled us to obtain much higher–quality spectra of individual galaxies. We compare the Mg II emission to the strengths and profiles of other emission lines, to better understand where this Mg II emission arises, and what its physical origins are.

2. SAMPLE AND OBSERVATIONS

[1] Astrophysics Science Division, Goddard Space Flight Center, 8800 Greenbelt Rd., Greenbelt, MD 20771
[2] Department of Physics, Harvard University, 17 Oxford St., Cambridge, MA 02138
[3] Harvard-Smithsonian Center for Astrophysics, 60 Garden St., Cambridge, MA 02138
[4] Department of Astronomy & Astrophysics, University of Chicago, 5640 S. Ellis Ave., Chicago, IL 60637
[5] Kavli Institute for Cosmological Physics, University of Chicago, 5640 South Ellis Ave., Chicago, IL 60637
[6] Department of Astronomy, University of Michigan, 500 Church St., Ann Arbor, MI 48109
[7] Max Plank Institute for Extraterrestrial Physics, Giessenbachstrasse 1, 85748 Garching, Germany
[8] Institute of Theoretical Astrophysics, University of Oslo, P.O. Box 1029, Blindern, NO-0315 Oslo, Norway

The data analyzed in this paper are part of a larger study of the rest-ultraviolet spectral properties of bright lensed galaxies, which we are conducting with the MagE spectrograph (Marshall et al. 2008) on the Clay Magellan II telescope. The galaxies discussed in this paper are the five from our larger sample that have redshifts such that both the Lyman α and Mg II 2796, 2803 features have spectral coverage. Four of the five galaxies discussed here are drawn from the SDSS Giant Arcs Sample (SGAS), a set of bright gravitationally lensed galaxies (Gladders et al. in prep; Bayliss et al. 2011, Bayliss 2012). The other galaxy, RCS0327 (Wuyts et al. 2010), comes from the Second Red Sequence Cluster Survey (Gilbank et al. 2011). Table 1 gives total integration times and dates of the observations. Further details of observations, data reduction, and full spectra will be published in future papers.

For RCS0327, we obtained MagE spectra for four distinct star-forming knots, labeled E, U, B, G, following the nomenclature of Sharon et al. (2012). The spectrum for Knot E has the highest signal-to-noise ratio.

3. RESULTS

3.1. *Systemic redshift*

For three galaxies, we measured systemic redshifts by fitting the C III] 1907, 1909 Å doublet with two Gaussians. The fit was constrained such that both lines shared a common linewidth. The redshift was allowed to vary, with the ratio of the central wavelengths held fixed.

S1441 lacks detected CIII] or other systemic lines; we therefore arbitrarily choose a systemic redshift of z=1.666, which puts the reddest Mg II 2796 Å absorption at zero velocity. RCS0327 has a complex velocity structure because it is undergoing a major merger (Wuyts et al. 2014). For Knot E of RCS0327 the C III] emission is blended with Fe II 2600 absorption from an intervening system at z=0.98295; we therefore instead use Si II* 1264, Si II* 1309, Si II* 1533, and Si III] 1882, finding a weighted-average emission line redshift of 1.7034 ± 0.00014 for Knot E. (This redshift is consistent within uncertainties with the section of the C III] profile that is not contaminated by intervening Fe II absorption.) Table 2 lists the measured systemic redshifts.

3.2. *Comparison of Lyα and Mg II emission strength*

Erb et al. (2012) reasoned that Mg II emission in z $\sim$ 1–2 galaxies should be similar to Lyman α emission, since both emission lines show P Cygni profiles, and since their emission strengths are generally correlated with UV color. However, since they lacked spectral coverage of Lyman α, they could not directly compare Mg II and Lyman α emission profiles or equivalent widths.

In Table 3 we report rest-frame equivalent widths and 2σ upper limits for emission lines. Reported uncertainties incorporate the statistical uncertainty as well as the systematic uncertainty due to continuum estimation. We determined the systematic uncertainty empirically by comparing continuum fitting methods; different methods agree well and have a standard deviation that is typically less than half the measurement uncertainty.

In Figure 1, we compare the equivalent widths of Mg II emission and Lyman α emission in our sample. The sample has reasonable dynamic range: the equivalent widths of Mg II vary by a factor of 6, and Lyman α by a factor of 8. No correlation is observed.

3.3. *Ubiquity of Mg II emission*

While the five galaxies in this paper were merely selected from our larger sample as spectral coverage of Mg II and Lyman α, in fact, all five show detected Mg II emission and absorption in a P Cygni profile. Mg II spectra are plotted in Figure 2. In §4 we explain why the ubiquity of Mg II emission in our sample is likely a selection effect.

3.4. *Velocity structure of the emission*

We now examine the velocity structure of the Mg II emission, compared to other prominent spectral features. Figure 2 presents velocity plots for these five lensed galaxies. Though RCS0327 has spectra measured for four knots, in Figure 2 we examine only the spectrum of Knot E, since it has the highest signal-to-noise ratio. (Detailed analysis of knot-to-knot variations in the Mg II profile within RCS0327 is reserved for a future paper.) Zero velocity corresponds to the systemic redshift of each galaxy, as determined in §3.1.

In each galaxy, the Mg II emission is broader than the C III] and [O II] lines, and the peak is redshifted with respect to systemic by 100 to 200 km s^{-1}. When Ly α is detected, it is even more redshifted than Mg II, with peak intensity at 200–250 km s^{-1} from systemic.

The red "shoulder" of Mg II 2796 Å emission will be absorbed by the 2803 Å transition. Thus, the 2803 Å line is the one to examine for redshifted emission. The Mg II profiles of S0108 and RCS0327 Knot E show a "shoulder" of emission extending $\sim$ 500 km s^{-1} redward of systemic. The Lyman α emission in S0108 and S0957 also show redshifted shoulders to even higher velocities (>600 km s^{-1}). Such extreme velocities imply a strong outflow. This result can be stated more generally: all the strong, high signal-to-noise Mg II and Lyman α emission lines in our sample show high-velocity red "shoulders".

4. DISCUSSION AND CONCLUSIONS

Mg II emission is present in all five of the gravitationally–lensed galaxies in our sample. This may seem surprising, given that Erb et al. (2012) find such emission in only one-third of their sample. An explanation may lie in the fact that Mg II emission is stronger in the Erb et al. stacked subsamples with lower stellar mass and bluer color; the reasons for this remain unclear. The lensed galaxies in our sample are quite blue. While we are still developing the lensing models required to infer intrinsic stellar mass for this sample, galaxies selected in a similar way have stellar masses around 10^9 M$_\odot$ (Wuyts et al. 2012), which would put them in the lower-mass bin of Erb et al., the bin that showed strongest Mg II emission. Lensed arc samples should be biased toward galaxies with high surface brightness features, in other words high specific star formation rates. Given the Erb et al. (2012) results, it is not surprising that the highly-magnified, high surface brightness star-forming regions captured within the MagE slit should show Mg II emission.

In RCS0327, the MagE spectra capture four different star-forming knots, but in the other four galaxies, the

MagE spectra capture only one bright knot of emission per galaxy. Past work shows that such knots typically extend only a few 100 pc (Wuyts et al. 2014; Sharon et al. 2012; Jones et al. 2012). In a future paper, we will examine the spatial variation of Mg II emission within RCS0327.

The lack of a correlation between the equivalent widths of Mg II and Lyman α emission is striking, and can be interpreted in several ways. Since Lyman α is a bluer transition with a higher absorption cross-section than Mg II, it can be expected to be more heavily obscured by dust. Galaxy-to-galaxy variations in extinction might erase an intrinsic correlation between Mg II and Lyman α emission, if present. A similar decoupling between UV continuum and Lyman α emission was proposed by (Giavalisco et al. 1996). An alternate explanation for the lack of correlation would be that Lyman α and Mg II emission do not share common origins. As a hydrogen recombination line, Lyman α originates in H II regions, and is then resonantly scattered. The origin of Mg II emission in distant galaxies is not well established; the two models proposed in the literature are intrinsic production of line emission in nebular regions with subsequent scattering, and intrinsic production of continuum photons that are resonantly scattered. Plasma models of H II regions (Cloudy, Ferland et al. 2013) predict weak nebular Mg II emission (Erb et al. 2012, their Figure 16); the dominant emission mechanism is the excitation of Mg^+ by electron impact (G. Ferland, priv. comm.) Thus, the flux of any *nebular* component of Mg II emission should be tied to the electron temperature and luminosity of the H II regions and the Lyman α flux, and not tied to the amount of Mg II absorption. A future study could test for a correlation between the extinction-corrected H α luminosity, which traces star formation rate, and the luminosity of Mg II emission.

Nebular Mg II emission is observed in the local universe, in the Orion H II region complex, as reviewed by Dufour (1987).[9] Torres-Peimbert et al. (1980) detected Mg II emission at low resolution with the International Ultraviolet Explorer (IUE) for a part of Orion; the flux of the emission was comparable to but less than C III] 1909. In high-resolution spectra of six regions of Orion, Boeshaar et al. (1982) find that the Mg II emission ranges from 0.04 to 1.35 times the strength of [O II] 2470 Å, and 0.25 to 25 times the strength of the C III] 1907,1909 Å doublet. By comparison, in our five galaxies, Mg II emission is much stronger than both [O II] 2470 and C III] 1907. These high line flux ratios argue against an intrinsically nebular origin for the bulk of the Mg II emission.

Mg II emission could also arise through the scattering of continuum photons that have the wavelength of the Mg II doublet, and are resonantly scattered through a velocity gradient until they emerge as Mg II emission. If the ultimate origin of Mg II emission is from continuum photons, then the equivalent width of Mg II emission should have no connection to that of Lyman α, but instead be tied to the Mg II absorbing column density and the characteristics of the outflowing wind. This could be examined in future work, for example by testing for a correlation between Mg II emission and the intrinsic Lyman α emission inferred from the observed fluxes of Lyman alpha and two Balmer lines.

The galaxies in our sample show a complex velocity structure in the emission components, with Mg II redshifted with respect to the nebular and Fe II* lines, and Lyman α (when present) even more redshifted, with a tail to more than 600 km s^{-1} from systemic. These observations can provide new insights into the wind structure of z$\sim$2 star-forming galaxies, through future multi-ion wind modeling. For now, it is enough to say that the Mg II emission does not have the velocity structure of either the nebular emission or the Lyman α emission. This suggests that the bulk of Mg II emission is emitted from physically different regions of the galaxy than is the nebular or Lyman α emission.

To conclude, the rest-ultraviolet spectra of five lensed galaxies presented here reveal that Mg II emission is not a simple proxy for Lyman α emission; its equivalent width is uncorrelated with that of Lyman α, and its velocity structure is different as well. Mg II emission, since it is bright and common in $z \sim 2$ galaxies, may prove to be a powerful diagnostic of winds driven by star formation in distant galaxies, once more work is done to understand its physical origin and radiative transfer.

Acknowledgments: This paper includes data gathered with the 6.5 meter Magellan Telescopes located at Las Campanas Observatory, Chile. Magellan time for this project was granted by the Carnegie Observatories, U. Michigan, U. Chicago, and the Harvard-Smithsonian Center for Astrophysics.

REFERENCES

Abazajian, K. N., et al. 2009, ApJS, 182, 543
Bayliss, M. B. 2012, ApJ, 744, 156
Bayliss, M. B., Hennawi, J. F., Gladders, M. D., et al. 2011, ApJS, 193, 8
Boeshaar, G. O., Harvel, C. A., Mallama, A. D., et al. 1982, NASA Conference Publication, 2338, 374
Dufour, R. J. 1987, Exploring the Universe with the IUE Satellite, 129, 577
Erb, D. K., Quider, A. M., Henry, A. L., & Martin, C. L. 2012, ApJ, 759, 26
Ferland, G. J., Porter, R. L., van Hoof, P. A. M., et al. 2013, Revista Mexicana de Astronomia y Astrofisica, 49, 137
Giavalisco, M., Vanzella, E., Salimbeni, S., et al. 2011, ApJ, 743, 95
Giavalisco, M., Koratkar, A., & Calzetti, D. 1996, ApJ, 466, 831
Gilbank, D. G., Gladders, M. D., Yee, H. K. C., & Hsieh, B. C. 2011, AJ, 141, 94
Jones, T., Stark, D. P., & Ellis, R. S. 2012, ApJ, 751, 51
Kinney, A. L., Bohlin, R. C., Calzetti, D., Panagia, N., & Wyse, R. F. G. 1993, ApJS, 86, 5
Koester, B. P., Gladders, M. D., Hennawi, J. F., et al. 2010, ApJ, 723, L73
Marshall, J. L., Burles, S., Thompson, I. B., et al. 2008, Proc. SPIE, 7014,

[9] Several authors (Rubin et al. 2011; Prochaska et al. 2011; Erb et al. 2012) have erroneously cited Kinney et al. (1993) as claiming that Mg II can be produced in H II regions. Kinney et al. in fact claimed no such detection, but rather adopted a list of emission lines seen in H II regions by IUE, as reviewed by Dufour (1987). The correct citations should be Torres-Peimbert et al. (1980) and Boeshaar et al. (1982), as reviewed by Dufour (1987). We note this to correct the citation stream.

TABLE 1
Log of Observations

source	t (hr)	UT date
SGAS J000451.7−010321	8.38	2010-12-09, 2013-08-10, 2013-10-06, 2013-10-07
SGAS J010842.2+062444	7.50	2012-08-19, 2012-08-20, 2012-09-14, 2013-08-10
RCSGA 032727−132609 knot E	10.0	2008-07-31, 2010-12-09, 2010-12-10
knot U	7.94	2008-07-31 , 2010-02-16, 2010-02-17, 2013-10-06, 2013-10-07
knot B	2.83	2013-10-06, 2013-10-07
knot G	1.83	2013-10-06, 2013-10-07
SGAS J095738.7+050929	2.08	2010-12-09, 2010-12-10
SGAS J144133.2−005401	1.50	2009-04-22

Note. — Source names, total integration times, and UT dates of observation. Full source names follow the convention of SGAS JHHMMSS.s±DDMMSS (Koester et al. 2010); abbreviated names (HHMM) are used subsequently.

TABLE 2
Systemic Redshifts

source	systemic redshift z_s	emission lines used for z_s
S0004	1.6811 ± 0.0001	C III] 1907/1909
S0108	1.91021 ± 0.00003	C III] 1907/1909
R0327 knotE	1.7034 ± 0.00014	Si II* 1264, 1309, 1533, Si III] 1882
S0957	1.82042 ± 0.00004	C III] 1907/1909

TABLE 3
Measured equivalent width of emission lines

source	2796	2803	Ly α	1907	1909	2326	2396	2470
S0004	-0.45 ± 0.1	-0.81 ± 0.17	-3.3 ± 0.4	-0.2 ± 0.1	-0.25 ± 0.1	> -0.26	> -0.26	> 0.26
S0108	-0.9 ± 0.6	-0.87 ± 0.25	-8.9 ± 0.6	-1.2 ± 0.1	-0.7 ± 0.1	-0.5 ± 0.1	-0.55 ± 0.15	> -0.30
R0327 knot E	-1.3 ± 0.16	-1.00 ± 0.17	> -1.2	-0.8 ± 0.1	-1.2 ± 0.1	-0.6 ± 0.15	-0.8 ± 0.15	-1.0 ± 0.1
knotB	-1.1 ± 0.5	-0.8 ± 0.3	> -2.5	-1.6 ± 0.4	-1.4 ± 0.35	> -0.7	> -0.8	-1.1 ± 0.35
knotG	-1.6 ± 0.6	-1.4 ± 0.6	> -3.8	> -1.1	> -1.05	> -0.96	-0.8 ± 0.4	> -0.75
knotU	-2.8 ± 0.3	-2.35 ± 0.2	> -1.1	-1.5 ± 0.1	-0.9 ± 0.1	-1.1 ± 0.4	-1.1 ± 0.2	-0.9 ± 0.1
S0957	-2.8 ± 0.9	-1.81 ± 0.77	-8.1 ± 1.2	-2.0 ± 0.3	-1.2 ± 0.3	> -0.87	> -0.71	> -0.85
S1441	-0.95 ± 0.4	> -0.8	> -3.4	> -0.62	> -0.62	> -1.0	> -1.2	> -0.92

Note. — Measured rest-frame equivalent width, in Å, of the following emission lines: Mg II 2796, Mg II 2803, Lyman α, C III] 1907, C III] 1909, C II] 2326, Fe II* 2396, [O II] 2470. For lines with P Cygni profiles, equivalent widths are of the emission component only. Two σ upper limits are quoted for non-detections.

Prochaska, J. X., Kasen, D., & Rubin, K. 2011, ApJ, 734, 24
Rubin, K. H. R., Prochaska, J. X., Ménard, B., et al. 2011, ApJ, 728, 55
Rubin, K. H. R., Weiner, B. J., Koo, D. C., et al. 2010, ApJ, 719, 1503
Sharon, K., Gladders, M. D., Rigby, J. R., et al. 2012, ApJ, 746, 161
Torres-Peimbert, S., Peimbert, M., & Daltabuit, E. 1980, ApJ, 238, 133
Weiner, B. J., Coil, A. L., Prochaska, J. X., et al. 2009, ApJ, 692, 187
Wuyts, E., Barrientos, L. F., Gladders, M. D., et al. 2010, ApJ, 724, 1182
Wuyts, E., Rigby, J. R., Gladders, M. D., & Sharon, K. 2014, ApJ, 781, 61
Wuyts, E., Rigby, J. R., Gladders, M. D., et al. 2012, ApJ, 745, 86

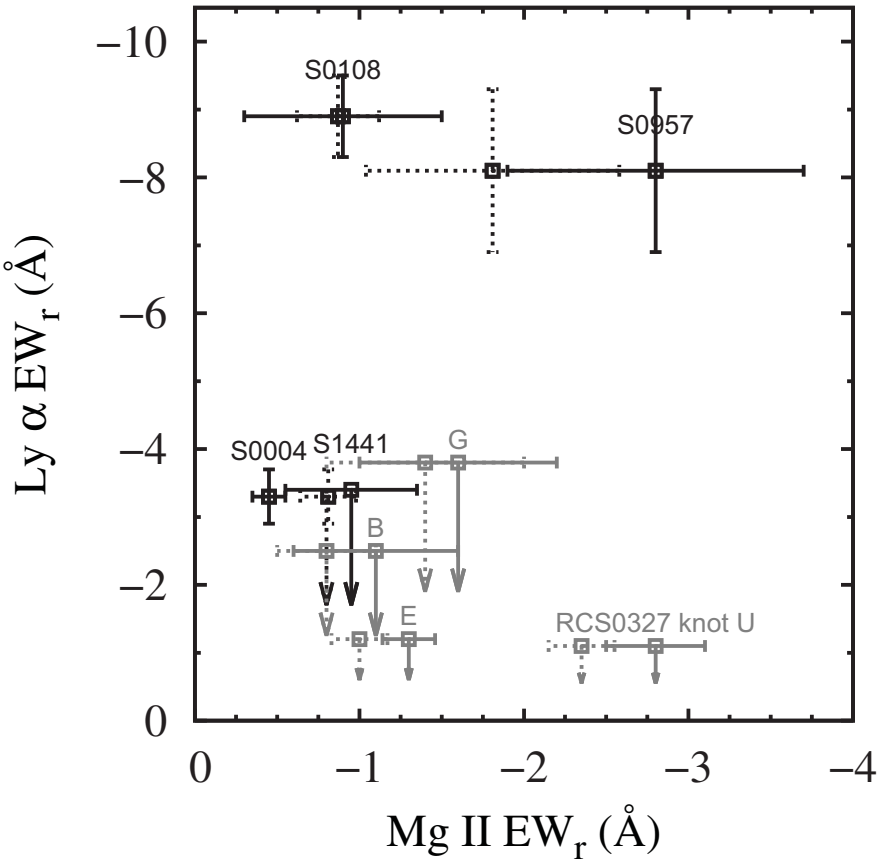

FIG. 1.— Rest-frame equivalenth width of Lyman α emission, as a function of the rest-frame equivalent widths of Mg II 2796 Å emission *(errorbars plotted as solid lines)*, and Mg II 2803 Å emission *(errorbars plotted with dotted lines)*. Values for each of four star-forming knots of RCS0327 are plotted in grey. The other galaxies are plotted in black. There is no apparent correlation between the equivalent widths of Mg II and Lyα.

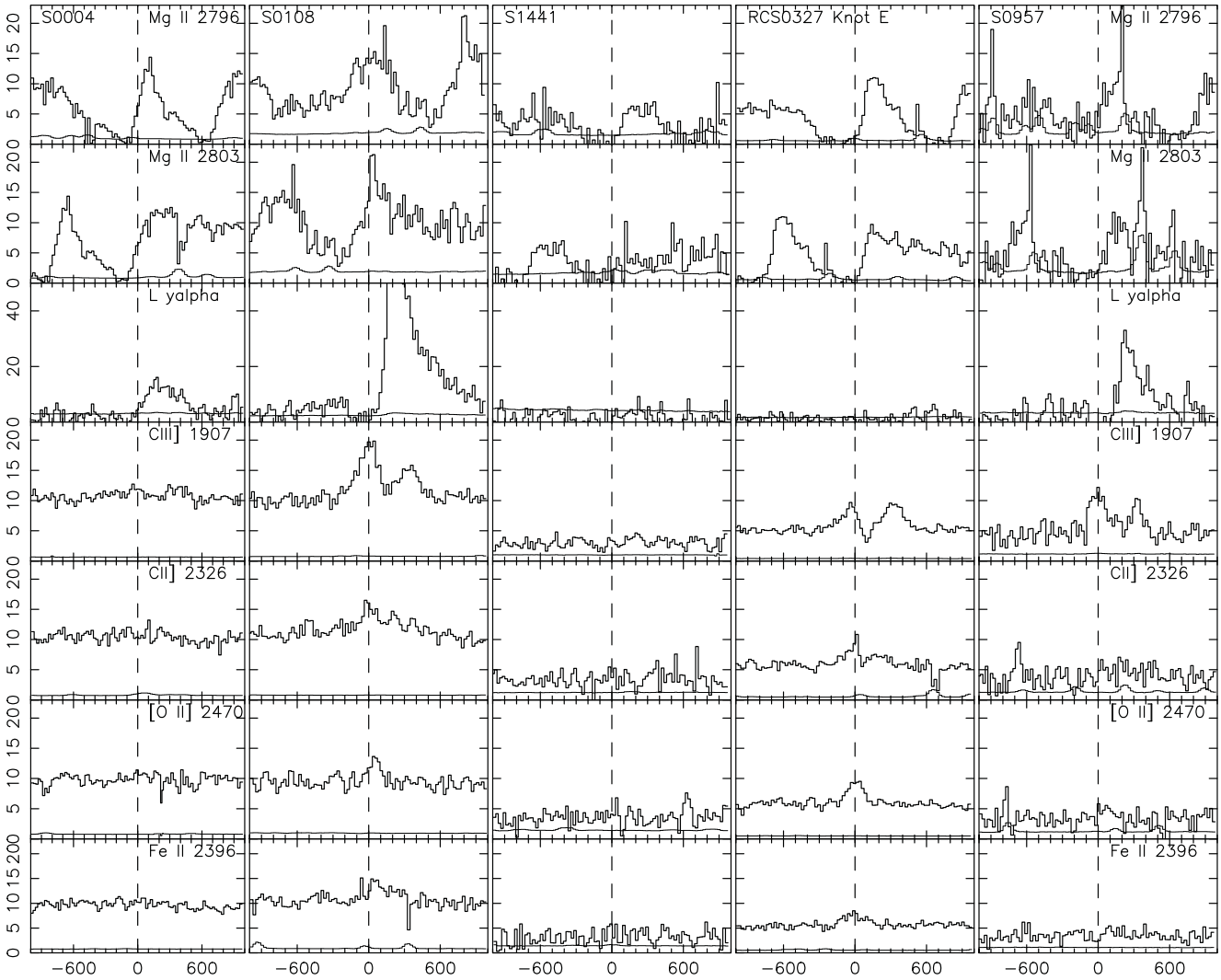

FIG. 2.— Velocity plots of spectral features in the MagE spectra of five lensed galaxies. Each column plots the spectrum of a different galaxy, labeled at top, as well as its 1σ uncertainty spectrum. The x-axis is velocity in km/s; zero velocity should be the systemic redshift. The y-axis is flux density in 1×10^{-29} erg s^{-1} cm^{-2} Hz^{-1}. Each row plots a different emission line, labeled at left and right. For RCS0327, only the spectrum of Knot E is shown.